Synthesis, Characterization, and Crystal Structure of a Vanadium(V)–Vanadium(IV)–Vanadium(V) Mixed-Valence Trinuclear Complex with a Tridentate Quinato Ligand, $(NH_4)_2\{[V^V(O)_2]_2[V^{IV}(O)](\mu\text{-}(-)\text{-quinato}(3-))_2\}\cdot H_2O$

Rachel Codd, Trevor W. Hambley, and Peter A. Lay*

Inorganic Chemistry Division, School of Chemistry, The University of Sydney, New South Wales 2006, Australia

Received August 18, 1994[⊗]

The synthesis, characterization, and crystal structure of the first mixed-valence V(V)–V(IV)–V(V) trinuclear complex is described. Crystals of $(NH_4)_2\{[V^V(O)_2]_2[V^{IV}(O)](\mu\text{-}(-)\text{-quinato}(3-))_2\}\cdot H_2O$ are monoclinic, space group $P2_1$, $a = 9.837(3)$ Å, $b = 8.180(3)$ Å, $c = 14.872(3)$ Å, $\beta = 99.65(3)°$, $Z = 2$, and $R = 0.022$ (678 F). Each trianion of quinic acid (1(*R*),3(*R*),4(*R*),5(*R*)-tetrahydroxycyclohexanecarboxylic acid) coordinates to all three vanadium ions. The ligand acts as a 2-hydroxylate chelate toward one V(V) ion and as a monodentate alcoholate toward the other V(V) ion. The alcoholate donors form a 1,3-diolato chelate and act as bridging groups between the central V(IV) ion and the outer V(V) ions. The geometry about all of the five-coordinate vanadium ions tends more toward an idealized square pyramid than toward a trigonal bipyramid, with the central V(IV) ion $[V(O)(OR')_2(OR'')_2]^{2-}$, having the most square-pyramidal character. The greater degree of trigonal character found in the coordination sphere of the V(V) centers $[V(O)_2(O_2CR)(OR')(OR'')]^{2-}$, compared to the V(IV) center, approximates the geometry of the active site of V(V) inhibitor complexes of enzymes, including ATPases and ribonucleases. The V=O bond lengths range between 1.611 and 1.624 Å. The bridging V(IV)–O(alcoholate) bond lengths range between 1.930 and 1.959 Å and are significantly shorter than the bridging V(V)–O(alcoholate) bond lengths, ranging between 1.984 and 2.041 Å, probably due to the steric constraints of the ligand. This is indicated by the much shorter terminal V(V)–O(carboxylate) bonds at 1.957 and 1.982 Å. The EPR spectrum ($g_{iso} = 1.9725$, $A_{iso} = 99.3 \times 10^{-4}$ cm^{-1}) is typical of a localized V(IV) system showing that the complex is a trapped-valence system. This is supported by a bond valence sum analysis (BVSA). The electronic spectrum shows a weak broad transition between 900 and 1000 nm, which is assigned to the intervalence transition of the complex.

Introduction

The last 20 years has witnessed a rapid expansion in interest in the bioinorganic chemistry of vanadium. The first biologically-important role assigned to vanadium was as an inhibitor of Na^+,K^+-ATPases and nucleases,[1] where V(V) adopted a distorted trigonal-bipyramidal geometry on binding to the active site of the enzymes. Subsequently, vanadium was found to be a cofactor in algal bromoperoxidases[2] and also bacterial nitrogenases.[3] Recent work has focused on the insulin-mimicking properties of vanadium.[4] While research over the last 20 years has uncovered many diverse roles played by vanadium in the bioinorganic arena, the exact role and details of the mechanisms of these systems are often not fully understood. This is partly due to the complexity inherent to vanadium solution chemistry, where speciation is dependent on vanadium concentration, pH, and available chelates. The most common oxidation states of vanadium, V(IV) and V(V), have both been implicated in biological systems and have been used as EPR and NMR probes, respectively, of the active sites of proteins and enzymes.[5] A more detailed understanding of the nature of vanadium and protein/enzyme interactions necessitates a detailed knowledge of the coordination environment and oxidation state of the metal(s) within the systems. Since both 1,2-diol and 2-hydroxy acid ligands produce V(V) complexes that structurally mimic the distorted trigonal-bipyramidal geometry in V(V)–protein inhibitor complexes,[1b,d,6a] it was of interest to prepare complexes of quinic acid, **I**, which combine both of these structural features.

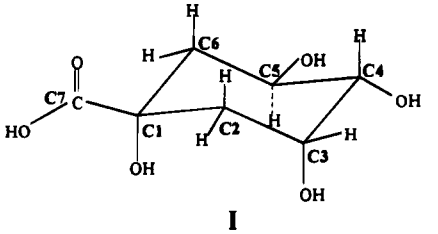

I

This ligand is found in coffee beans and is a precursor of shikimic acid, which is involved in the biosynthesis of essential aromatic amino acids.[7] The polyhydroxy-substituted cyclo-

[⊗] Abstract published in *Advance ACS Abstracts,* January 15, 1995.

(1) (a) Cantley, L. C.; Josephson, L.; Warner, R.; Yanagisawa, M.; Lechene, C.; Guidotti, G. *J. Biol. Chem.* **1977**, *252*, 7421–7423. (b) Lindquist, R. N.; Lynn, J. L., Jr.; Lienhad, G. E. *J. Am. Chem. Soc.* **1973**, *95*, 8762–8768. (c) Kostrewa, D.; Choe, H.-W.; Heinemann, U.; Saenger, W. *Biochemistry* **1989**, *28*, 7592–7600. (d) Borah, B.; Chen, C.; Egan, W.; Miller, M.; Wlodawer, A.; Cohen, J. S. *Biochemistry* **1985**, *24*, 2058–2067.

(2) Vilter, H. *Phytochemistry* **1984**, *23*, 1387–1390.

(3) Robson, R. L.; Eady, R. R.; Richardson, T. H.; Miller, R. W.; Hawkins, M.; Postgate, J. R. *Nature* **1986**, *322*, 388–390.

(4) (a) Shechter, Y.; Karlish, S. D. *Nature* **1980**, *284*, 556–558. (b) Posner, B. I.; Shaver, A.; Fantus, I. G. In *New Anti-Diabetic Drugs*; Bailey, C. J., Flatt, P. R., Eds.; Smith Gordon: London, 1990; pp 107–118.

(5) (a) Rehder, D. *Angew. Chem., Int. Ed. Engl.* **1991**, *30*, 148–167. (b) Chasteen, N. D. *Vanadium in Biological Systems*; Kluwer Academic Publishers: Dordrecht, The Netherlands, 1990.

(6) (a) Hambley, T. W.; Judd, R. J.; Lay, P. A. *Inorg. Chem.* **1992**, *31*, 343–345. (b) Judd, R. J. Ph.D. Thesis, University of Sydney, 1992. (c) Codd, R. B.Sc. Honours Thesis, University of Sydney, 1992. (d) Codd, R.; Field, L. D.; Hambley, T. W.; Judd, R. J.; Lay, P. A. *Inorg. Chem.*, to be submitted for publication.

0020-1669/95/1334-0877$09.00/0

hexane ring also has characteristics typical of a sugar molecule and, therefore, is of some interest in understanding complexes that may form between vanadium and sugars. Detailed studies of the binding of V(V) and polyhydroxy ligands have been restricted mainly to simple systems such as glycols and catechols.[8] Here, we report the isolation of an unusual mixed-valence V(V)−V(IV)−V(V) trinuclear complex, $(NH_4)_2\{[V^V(O)_2]_2[V^{IV}(O)](\mu\text{-}(-)\text{-quinato}(3-))_2\}\cdot H_2O$, with the 2-hydroxy acid (−)-quinic acid acting as a tridentate ligand, and a dinuclear V(V)−(−)-quinato complex, $(NH_4)_2[V^V(O)_2(\mu\text{-}(-)\text{-quinato}(2-))]_2\cdot 0.3CH_3CH_2OH$. While there have been many reports of mixed-valence $V^V{}_n-V^{IV}{}_m$ complexes[9,10] and polynuclear V(IV)[11] and V(V)[12,13] structures, this appears to be the first reported structure of a mixed-valence V(V)−V(IV)−V(V) trinuclear complex.

Experimental Section

Physical Measurements. UV−vis spectra were obtained on a Hewlett-Packard 8452A diode array spectrophotometer utilizing the HP 89531A UV−vis operating software for data collection. Electronic spectra in the near-IR region (both in solution and in the solid state) were recorded on a Cary 5E UV/vis/near-IR spectrophotometer. The broad spectral band in the visible region was deconvoluted using the GRAMS program within the Win-IR software (Bio-Rad). The diffuse reflectance measurements, in a KBr matrix, were performed using the Cary 5E modified Harrick diffuse reflectance accessory. Circular dichroism spectra were collected on a Jasco J-500C spectropolarimeter using a sensitivity of 5 mdeg cm^{-1} and a time constant of 1 s. The baseline was corrected by subtracting background spectra. Fourier transform infrared (FTIR) spectra were recorded on a Bio-Rad FTS-7 FTIR spectrometer. Magnetic susceptibility measurements were obtained using a Sherwood Scientific magnetic susceptibility balance. The apparatus was calibrated with $(NH_4)_2Fe(SO_4)_2\cdot 6H_2O$ (Merck), and diamagnetic corrections for the constituent atoms were calculated using a standard source.[14] Room-temperature X-band EPR spectra (*ca.* 9.6 GHz) were recorded in quartz flat cells using a Bruker ESP300 spectrometer linked to a Hewlett Packard 5352B microwave frequency counter and a Bruker ERO35M NMR gaussmeter. Second-order corrections were applied to spectral calculations. Microanalyses were performed by the Australian National University Microanalytical Service. NMR spectra were obtained on a Bruker (AC200F) spectrometer operating at 200.13 MHz for proton [reference: sodium 3-(trimethylsilyl)-1-propanesulfonate] and 50.23 MHz for carbon [reference: dioxane].

Syntheses. $(NH_4)_2[V^V(O)_2(\mu\text{-}(-)\text{-quinato}(2-))]_2\cdot 0.3CH_3CH_2OH$ (II). An aqueous solution (20 mL) of quinic acid (ICN Biomedical, 4.701 g, 24.3 mmol) was neutralized with ammonia, and V_2O_5 (Merck, extra pure) was added (2.224 g, 12.28 mmol) in small aliquots over a $^1/_2$ h period. The solution was heated slightly, <40 °C, and was filtered to remove trace amounts of unreacted V_2O_5. The volume of the solution was reduced to 15 mL via rotary evaporation (external bath 40 °C). Ethanol (250 mL) was added to the concentrate with vigorous swirling, forming a finely divided yellow powder, which was filtered off, washed with ethanol (50 mL), and dried *in vacuo* over silica gel overnight. Yield: 3.36 g (47.6%). Anal. Calcd for $C_{14.6}H_{29.8}N_2O_{16.3}V_2$: C, 29.42; H, 5.04; N, 4.70; V, 17.09. Found: C, 29.23; H, 5.59; N, 4.31; V, 17.45. FTIR (KBr matrix): 3200 (s, br), 3050 (m, br), 1630 (s, br), 1429 (m), 1341 (m), 1152 (w), 1119 (m), 1069 (m), 994 (sh), 966 (m), 945 (m), 814 (m), 762 (m), 687 (m), 617 (m) cm^{-1}. UV−vis (H_2O) λ, nm (ϵ, $M^{-1}\,cm^{-1}$): 210 (8.3×10^3), 258 (3.3×10^3). δ_H (200 MHz, D_2O): 1.14, t (solvent CH_3CH_2OH); 1.84, AB quartet, J = 11.7 Hz (H2e); 2.04, multiplet (H2a, H5a, H5e); 3.52, AX doublet of doublets, J = 9.8 Hz (H4); 3.6, quartet (solvent CH_3CH_2OH); 4.0, doublet of quartets, broad (H3); 4.1, quartet, broad (H5); 4.4, multiplet, broad. The integration of the EtOH peak in the NMR confirmed the structural formulation. δ_C (50 MHz, D_2O): 16.71 (solvent CH_3CH_2OH); 36.81, 38.92 (C2); 40.63, 41.89 (C6); 57.31 (solvent CH_3CH_2OH); 66.73 (C5); 70.48 (C3); 75.13 (C4); 77.15 (C6); 183.42 (C7).

$(NH_4)_2\{[V^V(O)_2]_2[V^{IV}(O)](\mu\text{-}(-)\text{-quinato}(3-))_2\}\cdot H_2O$. The pH of the aqueous ethanolic filtrate of **II** obtained above was adjusted with dilute HCl from 5.6 to 3.3, whereupon small blue crystals appeared after 1 week. The blue crystals were filtered off and recrystallized from water/ethanol using vapor diffusion. Microanalysis indicated a trinuclear structure (Anal. Calcd for $C_{14}H_{28}N_2O_{18}V_3$: C, 25.28; H, 4.24; N, 4.21. Found: C, 25.24; H, 4.30; N, 4.24). These crystals were used for the crystallographic analysis. A subsequent synthesis gave a higher yield of the trinuclear title complex using 3.079 g (16.0 mmol) of quinic acid and 1.456 g (8.0 mmol) of V_2O_5. The finely divided yellow complex, **II**, was prepared as described above and removed by filtration, and the filtrate was retained. The solid was redissolved in the minimum amount of water and extracted into ethanol (60 mL), and the extract was filtered. The pH of the aqueous ethanolic solution was adjusted to 3.3 and the solution left to stand for 1 week. The well-formed blue needle-shaped crystals formed after this time were filtered off and recrystallized from water/ethanol, using vapor diffusion. Final yield: 0.648 g (23%). FTIR (KBr matrix): 3476 (w), 3280 (m, br), 3025 (m), 1665 (m), 1431 (m), 1341 (m), 1312 (w), 1283 (w), 1152 (w), 1107 (m), 1083 (w), 1042 (w), 1011 (w), 970 (m), 932 (s), 864 (w), 837 (m), 758 (w), 706 (w), 681 (w), 619 (w), 571 (m), 540 (w), 504 (m) cm^{-1}. The FTIR spectrum was identical to that of the first crop of blue crystals obtained above. UV−vis (water) λ, nm (ϵ, $M^{-1}\,cm^{-1}$): 220 (8.08×10^3), 260 sh (4.63×10^3), broad band between 500 and 700 nm comprising three bands at 521 (2.6), 560 (5.7), and 629 (10.0), 810 (1.8), 960, br (<1). CD (water) λ, nm ($10^2\epsilon$, deg $M^{-1}\,m^{-1}$): 284 (−19.9), 338 (+7.7), 521 (−1.6), 560 (−1.2), 629 (−0.3).

X-ray Crystallography. For diffractometry, the crystal was mounted on a glass fiber with cyanoacrylate resin. Lattice parameters at 21 °C were determined by least-squares fits to the setting parameters of 25 independent reflections, measured and refined on an Enraf-Nonius CAD4-F four-circle diffractometer employing graphite-monochromated Mo Kα radiation. Intensity data were collected in the range $1 < \theta < 25°$. Data reduction and application of Lorentz, polarization, absorption, and decomposition corrections were carried out using the teXsan system.[15] The structure was solved by direct methods using SHELXS-86,[16] and the solution was extended by difference Fourier methods. Hydrogen atoms in $(NH_4)_2\{[V^V(O)_2]_2[V^{IV}(O)](\mu\text{-}(-)\text{-quinato}(3-))_2\}\cdot H_2O$ were included at calculated sites (C−H, N−H 0.97 Å) with individual isotropic thermal parameters. All other atoms were refined anisotropically. Full-matrix least-squares methods were used to refine an overall scale factor and positional and thermal parameters. Neutral atom scattering factors were taken from Cromer and Waber.[17] Anomalous dispersion effects were included in F_c;[18] the values for $\Delta f'$ and $\Delta f''$ were those of Creagh and McAuley.[19] The values for the

(7) (a) Bohm, B. A. *Chem. Rev.* **1965**, *65*, 435−466. (b) Kelley, C. J.; Harruff, R. C.; Carmack, M. *J. Org. Chem.* **1976**, *41*, 449−455. (c) Corse, J.; Lundin, R. E.; Sondheimer, E.; Waiss, A. C., Jr. *Phytochemistry* **1966**, *5*, 767−776.
(8) Boyd, D. B.; Kustin, K. *Adv. Inorg. Biochem.* **1984**, *6*, 312−365.
(9) Young, C. G. *Coord. Chem. Rev.* **1989**, *96*, 89−251.
(10) (a) Babonneau, F.; Sanchez, C.; Livage, J.; Launay, J. P.; Daoudi, M.; Jeannin, Y. *Nouv. J. Chim.* **1982**, *6*, 353−358. (b) Jeannin, Y.; Launay, J. P.; Seid Sedjadi, M. A. *J. Coord. Chem.* **1981**, *11*, 27−34. (c) Riechel, T. L.; Sawyer, D. T. *Inorg. Chem.* **1975**, *14*, 1869−1875. (d) Nishizawa, M.; Hirotsu, K.; Ooi, S.; Saito, K. *J. Chem. Soc., Chem. Commun.* **1979**, 707−708.
(11) Chakravarty, J.; Dutta, S.; Chakravorty, A. *J. Chem. Soc., Dalton Trans.* **1993**, 2857−2858.
(12) Ishaque Khan, M.; Chen, Q.; Zubieta, J. *J. Chem. Soc., Chem. Commun.* **1992**, 305−306.
(13) (a) Hillerns, F.; Olbrich, F.; Behrens, U.; Rehder, D. *Angew. Chem., Int. Ed. Engl.* **1992**, *31*, 447−448. (b) Crans, D. C.; Marshman, R. W.; Gottlieb, M. S.; Anderson, O. P.; Miller, M. M. *Inorg. Chem.* **1992**, *31*, 4939−4949. (c) Crans, D. C.; Felty, R. A.; Anderson, O. P.; Miller, M. M. *Inorg. Chem.* **1993**, *32*, 247−248. (d) Mokry, L. M.; Carrano, C. J. *Inorg. Chem.* **1993**, *32*, 6119−6121. (e) Pecoraro, V. L. *Inorg. Chim Acta* **1989**, *155*, 171−173. (f) Crans, D. C.; Felty, R. A; Miller, M. M. *J. Am. Chem. Soc.* **1991**, *113*, 265−269.
(14) Mabbs, F. E.; Machin, D. J. In *Magnetism and Transition Metal Complexes*; Chapman and Hall: London, 1973.
(15) teXsan, Crystal Structure Analysis Package, Molecular Structure Corp. (1985, 1992).
(16) Sheldrick, G. M. SHELXS-86. *Crystallographic Computing 3*; Sheldrick, G. M., Kruger, C., Goddard, R., Eds.; Oxford University Press: Oxford, England, 1985; pp 175−189.
(17) Cromer, D. T.; Waber, J. T. *International Tables for X-Ray Crystallography*; Kynoch Press: Birmingham, England, 1974; Vol. IV.
(18) Ibers, J. A.; Hamilton, W. C. *Acta Crystallogr.* **1964**, *17*, 781−782.

Table 1. Crystallographic Data for $(NH_4)_2\{[V^V(O)_2]_2[V^{IV}(O)](\mu\text{-}(-)\text{-quinato}(3-))_2\}\cdot H_2O$

chem formula	$C_{14}H_{28}O_{18}N_2V_3$	fw	665.20
crystal system	monoclinic	space group	$P2_1$
a	9.837(3) Å	T	21 °C
b	8.180(3) Å	λ	0.710 69 Å
c	14.872(3) Å	ϱ_{calcd}	1.873 g cm^{-3}
β	99.65(2)°	μ	9.962 cm^{-1}
V	1179.7 Å^3	R^a	0.022
Z	2	$R_w{}^b$	0.022

$^a R = \Sigma||F_o| - |F_c||/|F_o|$. $^b R_w = [\{w(|F_o| - |F_c|)^2\}/\{w|F_o|^2\}]^{1/2}$.

Table 2. Positional and Thermal Parameters for $(NH_4)_2\{[V^V(O)_2]_2[V^{IV}(O)](\mu\text{-}(-)\text{-quinato}(3-))_2\}\cdot H_2O$

atom	x	y	z	B_{eq},[a] Å^2
V1	0.798248(61)	0.233	0.870322(37)	1.81(2)
V2	0.316115(59)	0.25105(12)	0.630527(37)	1.67(2)
V3	0.607071(56)	0.40066(12)	0.706865(36)	1.30(2)
O1	0.66324(26)	0.56412(35)	0.66503(17)	1.9(1)
O2	0.64822(22)	0.39774(38)	0.84019(14)	1.7(1)
O3	0.75997(22)	0.24908(36)	0.73290(14)	1.7(1)
O4	0.41367(22)	0.43362(33)	0.70994(14)	1.5(1)
O5	0.51186(22)	0.25271(38)	0.61342(14)	1.6(1)
O6	0.30094(29)	0.06493(39)	0.66294(20)	3.1(1)
O7	0.24080(26)	0.26534(47)	0.52495(16)	3.2(1)
O8	0.91904(27)	0.34063(37)	0.92947(17)	2.7(1)
O9	0.72559(33)	0.12343(40)	0.93931(20)	3.2(1)
O10	0.90796(29)	0.05136(39)	0.83087(17)	3.0(1)
O11	0.94975(30)	-0.11341(42)	0.72224(18)	3.5(1)
O12	0.84489(28)	0.31580(40)	0.46024(18)	2.4(1)
O13	0.55879(24)	0.26628(36)	0.42873(15)	2.0(1)
O14	0.17035(25)	0.35035(40)	0.68715(18)	3.0(1)
O15	0.10679(26)	0.51445(44)	0.79001(18)	3.2(1)
O16	0.50224(34)	0.89905(44)	0.86274(21)	2.9(1)
O17	0.70712(32)	0.68309(43)	0.95525(23)	2.5(1)
N1	0.03188(52)	0.20114(57)	0.09956(30)	2.8(2)
N2	0.95666(35)	−0.38223(49)	0.60285(23)	2.9(2)
C1	0.79412(36)	0.11343(48)	0.67973(23)	1.7(1)
C2	0.66553(42)	0.01629(53)	0.64163(28)	1.7(2)
C3	0.56838(36)	0.11389(48)	0.57126(23)	1.5(1)
C4	0.64269(38)	0.17075(51)	0.49458(25)	1.7(1)
C5	0.76942(36)	0.26924(51)	0.53123(23)	1.7(1)
C6	0.86726(39)	0.17367(54)	0.60164(26)	1.9(2)
C7	0.89236(39)	0.00559(53)	0.74704(27)	2.3(2)
C8	0.35007(38)	0.49343(49)	0.78415(24)	1.6(1)
C9	0.41081(39)	0.39834(59)	0.87063(24)	1.9(1)
C10	0.55989(39)	0.44663(49)	0.90418(25)	1.7(2)
C11	0.57043(39)	0.63027(54)	0.92319(25)	1.9(2)
C12	0.51341(38)	0.73044(54)	0.83936(24)	1.9(1)
C13	0.36913(42)	0.67528(53)	0.79761(30)	1.9(2)
C14	0.19686(37)	0.45205(52)	0.75459(25)	2.0(2)
O18	0.77153(37)	0.52785(56)	0.12337(22)	5.6(2)

$^a B_{eq} = {}^8/_3\pi^2[U_{11}(aa^*)^2 + U_{22}(bb^*)^2 + U_{33}(cc^*)^2 + 2U_{12}aa^*bb^* \cos\gamma + 2U_{13}aa^*cc^* \cos\beta + 2U_{23}bb^*cc^* \cos\alpha]$.

mass attenuation coefficients are those of Creagh and Hubbel.[20] All calculations were performed using the teXsan[15] crystallographic software package of the Molecular Structure Corp., and plots were drawn using ORTEP.[21] The crystallographic data are summarized in Table 1. Non-hydrogen atom coordinates are listed in Table 2. The atomic nomenclature is defined in Figure 1. Listings of bond lengths and angles are given in Tables 3 and 4. Listings of H atom coordinates, anisotropic thermal parameters, close intermolecular contacts, and torsion angles and a unit cell packing diagram (Tables S1−S6, Figure S1) have been deposited as supplementary material.

(19) Creagh, D. C.; McAuley, W. J. In *International Tables for Crystallography*; Wilson, A. J. C., Ed.; Kluwer Academic Publishers: Boston, MA, 1992; Vol. C, Table 4.2.6.8, pp 219−222.

(20) Creagh, D. C.; Hubbell, J. H. In *International Tables for Crystallography* Wilson, A. J. C., Ed.; Kluwer Academic Publishers: Boston, MA, 1992; Vol. C, Table 4.2.4.3, pp 200−206.

(21) Johnson, C. K. *ORTEP: A Thermal Ellipsoid Plotting Program*; Oak Ridge National Laboratory: Oak Ridge, TN, 1965.

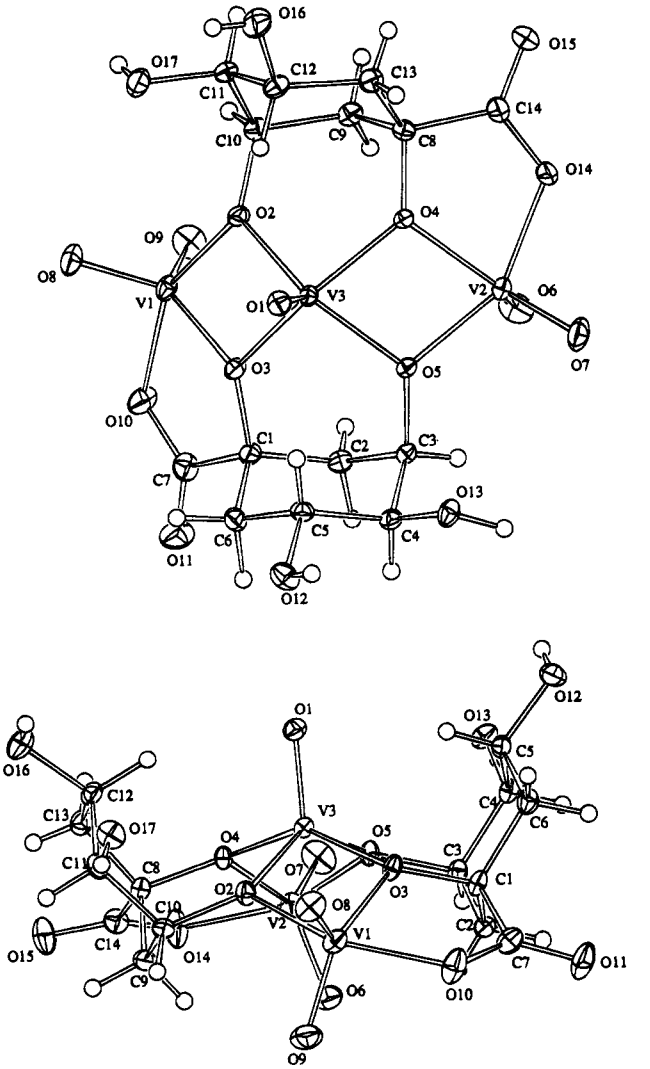

Figure 1. ORTEP plot of the complex anion $\{[V^V(O)_2]_2[V^{IV}(O)](\mu\text{-}(-)\text{-quinato}(3-))_2\}^{2-}$ giving the crystallographic atom numbering. 30% probability ellipsoids are shown: (a) view down the V(IV)−O(oxo) bond; (b) view normal to the V(IV)−O(oxo) bond.

Table 3. Bond Lengths (Å) for $\{[V^V(O)_2]_2[V^{IV}(O)](\mu\text{-}(-)\text{-quinato}(3-))_2\}^{2-}$

V1−O2	1.994(3)	V1−O3	2.019(2)
V1−O8	1.616(3)	V1−O9	1.616(3)
V1−O10	1.982(3)	V2−O6	1.611(3)
V2−O4	2.041(2)	V2−O5	1.984(2)
V2−O7	1.624(2)	V2−O14	1.957(3)
V3−O1	1.611(3)	V3−O2	1.956(2)
V3−O3	1.938(3)	V3−O4	1.930(2)
V3−O5	1.959(2)	O2−C10	1.448(4)
O3−C1	1.435(4)	O4−C8	1.442(4)
O5−C3	1.452(4)	O15−C14	1.217(4)
O16−C12	1.431(5)	O13−C4	1.407(4)
O10−C7	1.286(4)	O11−C7	1.213(5)
O17−C11	1.417(5)	O12−C5	1.440(4)
O14−C14	1.295(4)	C3−C4	1.527(5)
C1−C2	1.520(5)	C1−C7	1.546(5)
C2−C3	1.520(5)	C1−C6	1.546(5)
C4−C5	1.507(5)	C5−C6	1.516(5)
C8−C9	1.536(5)	C8−C13	1.508(6)
C8−C14	1.535(5)	C9−C10	1.520(5)
C10−C11	1.529(6)	C11−C12	1.519(5)
C12−C13	1.519(5)		

Results

Syntheses. The reaction of V_2O_5 in aqueous ammonia with quinic acid in a 1:2 molar ratio (equimolar concentrations of V and ligand) results in a yellow precipitate upon the addition of ethanol, which analyzed as $(NH_4)_2[V^V(O)_2(\mu\text{-})\text{-quinato-}$

Table 4. Selected Bond Angles (deg) for $\{[V^{V}(O)_2]_2[V^{IV}(O)](\mu\text{-}(-)\text{-quinato}(3-))_2\}^{2-}$

O2−V1−O3	73.90(9)	O2−V3−O5	134.8(1)
O2−V1−O8	101.7(1)	O3−V3−O4	145.1(1)
O2−V1−O9	97.4(1)	O3−V3−O5	90.5(1)
O2−V1−O10	149.3(1)	O4−V3−O5	75.36(9)
O3−V1−O8	120.7(1)	V1−O2−V3	104.8(1)
O3−V1−O9	130.7(1)	V1−O2−C10	122.8(2)
O3−V1−O10	76.6(1)	V3−O2−C10	128.1(2)
O8−V1−O9	108.6(2)	V1−O3−V3	104.5(1)
O8−V1−O10	100.5(1)	V1−O3−C1	119.1(2)
O9−V1−O10	95.4(2)	V3−O3−C1	129.1(2)
O4−V2−O5	72.37(9)	V2−O4−V3	104.7(1)
O4−V2−O6	125.2(1)	V2−O4−C8	118.0(2)
O4−V2−O7	126.9(2)	V3−O4−C8	128.4(2)
O4−V2−O14	75.8(1)	V2−O5−V3	105.8(1)
O5−V2−O6	100.7(1)	V2−O5−C3	120.0(2)
O5−V2−O7	99.8(1)	V3−O5−C3	128.1(2)
O5−V2−O14	148.1(1)	V1−O10−C7	121.5(2)
O6−V2−O7	107.9(2)	V2−O14−C14	122.2(2)
O6−V2−O14	98.8(1)	O3−C1−C2	110.6(3)
O7−V2−O14	97.9(1)	O3−C1−C6	110.4(3)
O1−V3−O2	112.1(1)	O3−C1−C7	105.3(3)
O1−V3−O3	107.7(1)	C2−C1−C6	110.5(3)
O1−V3−O4	107.2(1)	C2−C1−C7	109.5(3)
O1−V3−O5	113.1(1)	C6−C1−C7	110.4(3)
O2−V3−O3	76.6(1)	C1−C2−C3	111.7(3)
O2−V3−O4	90.86(9)	O5−C3−C2	110.8(3)
O5−C3−C4	110.5(3)	O16−C12−C13	106.3(3)
C2−C3−C4	110.5(3)	C11−C12−C13	111.5(3)
O13−C4−C3	113.0(3)	C8−C13−C12	115.7(4)
O13−C4−C5	107.9(3)	O14−C14−O15	122.6(3)
C3−C4−C5	111.3(3)	O14−C14−C8	115.1(3)
O12−C5−C4	111.9(3)	O15−C14−C8	122.3(4)
O12−C5−C6	107.3(3)	C4−C5−C6	111.4(3)
C1−C6−C5	111.2(3)	O10−C7−O11	122.8(4)
O10−C7−C1	114.9(3)	O11−C7−C1	122.2(3)
O4−C8−C9	108.1(3)	O4−C8−C13	112.1(3)
O4−C8−C14	103.7(3)	C9−C8−C13	111.5(3)
C9−C8−C14	110.7(3)	C13−C8−C14	110.4(3)
C8−C9−C10	111.2(3)	O2−C10−C9	111.4(3)
O2−C10−C11	111.3(3)	C9−C10−C11	110.3(3)
O17−C11−C10	113.1(3)	O17−C11−C12	108.1(3)
C10−C11−C12	112.0(3)	O16−C12−C11	110.7(3)

Table 5. ^{1}H-Decoupled ^{13}C NMR Spectral Shifts (ppm) of **I** and **II** in D_2O[a]

I	36.5	40.0	66.1	69.8	74.6	75.4	177.5
II	36.8	40.6	66.7	70.5	75.1	77.1	183.4
	38.9[b]	41.9[b]					
assign	C2	C6	C5	C3	C4	C1	C7

[a] This work and ref 7b. [b] The resonances observed here suggest a mixture of species is present.

$(2-))]_2 \cdot 0.3CH_3CH_2OH$, **II**. The complex is diamagnetic and EPR silent. Electronic spectral data and ^{1}H and ^{13}C NMR data (Table 5) suggest that the major species present has a dinuclear structure Similar to that observed for analogous 2-hydroxy acid complexes, **III**, which have been prepared by a similar method[22] and characterized by X-ray crystallography.[6]

Repeated attempts to grow crystals of **II** suitable for X-ray crystallography, however, have been unsuccessful. While the properties and microanalyses are consistent with the proposed structure, the features in the FTIR spectra are broad, which suggests a mixture of species may be present. Broad resonances are also observed in the NMR spectra of the complex, again suggesting a mixture of species may be present in solution and/or there is an equilibrium between species.

The blue mixed-valence trinuclear complex $(NH_4)_2\{[V^{V}(O)_2]_2[V^{IV}(O)](\mu\text{-}(-)\text{-quinato}(3-))_2\}\cdot H_2O$ formed when an ethanolic solution of **II** was acidified and allowed to stand over 1 week.

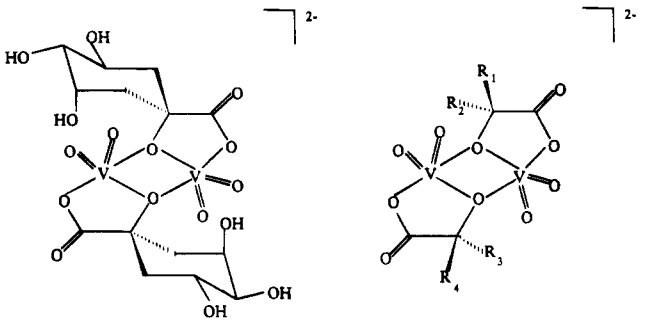

II **III**

X-ray Structure of $(NH_4)_2\{[V^{V}(O)_2]_2[V^{IV}(O)](\mu\text{-}(-)\text{-quinato}(3-))_2\}\cdot H_2O$. Tables 3 and 4 list the bond lengths and selected bond angles, respectively, of the anion of $(NH_4)_2\{[V^{V}(O)_2]_2[V^{IV}(O)](\mu\text{-}(-)\text{-quinato}(3-))_2\}\cdot H_2O$, and an ORTEP plot of the complex with the atom-labeling scheme is shown in Figure 1. The complex consists of an oxovanadium(IV) center (V3) with two dioxovanadate(V) groups at either side (V1, V2). The three vanadium atoms are linked via two quinic acid ligands acting in a tridentate fashion. The deprotonated carboxyl group coordinates to an outer V(V) ion (V1). The hydroxyl group on C1 donates a bridging oxygen (O3) between the same outer V(V) and the V(IV) center (V3), forming a stable five-membered ring, with respect to V1. The hydroxyl group on C3 donates a bridging oxygen (O5) between the opposite outer V(V) (V2) and the V(IV) center, forming a six-membered ring comprised of the atoms C1, O3, V3, O5, C3, and C2. The second (−)-quinato(3−) ligand is coordinated in the same fashion, albeit "flipped", giving the complex a pseudosymmetry. Both quinic acid ligands adopt chair conformations. The degree of trigonality of each five-coordinate vanadium ion can be defined by the parameter τ as discussed by Addison *et al.*,[23] where τ is a function of the two greatest basal plane angles. An idealized square-pyramidal geometry has $\tau = 0$, which tends toward unity with the increasing degree of trigonality. The τ values in $(NH_4)_2\{[V^{V}(O)_2]_2[V^{IV}(O)](\mu\text{-}(-)\text{-quinato}(3-))_2\}\cdot H_2O$ are 0.31 (V1), 0.35 (V2), and 0.17 (V3), indicating that the geometries of all three vanadium centers show more square-pyramidal than trigonal character with the vanadyl center having the most square-pyramidal character.

All of the V=O bond lengths (1.611−1.624 Å) lie within the range observed for other oxovanadium complexes.[24] The two central V−O−V−O planes of the molecule lie at a dihedral angle of 119.5°. The V−O−V angles average 105°, similar to the V−O−V angles of 104° reported by Crans *et al.* for a tetranuclear oxo-bridged V(V) cluster.[13b]

The bond lengths of the bound ligand do not differ appreciably from those found in free quinic acid.[25] Significant differences are found, however, when the bond angles in the free ligand are compared with the corresponding bond angles in the complex, where the ligand is acting as a tridentate chelate. The angles bounded by the tertiary alcoholate oxygens and the carboxylate carbons [ring 1, O3−C1−C7 = 105.3(3)°; ring 2, O4−C8−C14 = 103.7(3)°] in the complex, are 6.6 and 8.2° smaller, respectively, than the same angle in the free ligand [111.9(1)°]. This increase in strain is a result of the formation of the five-membered ring about the V(V) ions. A smaller decrease (3°) in the cyclohexane ring angles C1−C2−C3 [111.7(3)°] and C10−C9−C8 [111.2(3)°] compared to the corresponding angle in the free ligand [114.4(1)°] can be

(22) Harnung, S. E.; Larsen, E.; Pedersen, E. J. *Acta Chem. Scand.* **1993**, *47*, 674−682.

(23) Addison, A. W.; Rao, T. N.; Reedijk, J.; van Rijn, J.; Verschoor, G. C. *J. Chem. Soc., Dalton Trans.* **1984**, 1349−1356.

(24) Holloway, C. E.; Melnik, M. *Rev. Inorg. Chem.* **1985**, *7*, 75−159.

(25) Abell, A.; Allen, F. H.; Bugg, T. D. H.; Doyle, M. J.; Raithby, P. R. *Acta Crystallogr., Sect. C* **1988**, *C44*, 1287−1290.

explained as a result of the diol bite. A unit cell packing diagram reveals four intramolecular hydrogen bonds and two intermolecular hydrogen bonds per unit cell. The intramolecular hydrogen bonds occur between the hydroxy moieties on C4 and C5 (and C11 and C12) within each molecule. The intermolecular hydrogen bonding involves the V(IV) oxo group (molecule 1) and the H atom on O12 (molecule 2) and a V(V) oxo group (molecule 2) and the same hydrogen on the opposite molecule (molecule 1).

Spectroscopy. The FTIR spectra of both oxovanadium complexes isolated here have sharp bands in the 950−1000 cm^{-1} region representing the V=O stretch.[24] Complex **II** has a single band at 998 cm^{-1}, while the mixed-valence trinuclear complex has bands at 968 and 1012 cm^{-1}, which are tentatively assigned to the V=O stretches of the different oxidation states. Both complexes have a strong band at 1650 cm^{-1} representing the antisymmetric stretch of the monodentate carboxyl moiety with the symmetric stretch of this same functional group observed at 1341 cm^{-1}.

The electronic spectra of dinuclear dioxovanadate complexes with 2-hydroxy acid ligands, **II** and **III**, feature an absorption in the UV (λ_{max} = 258 nm)[6,22] which tails off in the visible region of the spectrum, since there are no d electrons in the outer shell of a V(V) configuration. The electronic spectrum of $(NH_4)_2\{[V(O)_2]_2[V^{IV}(O)](\mu\text{-}(-)\text{-quinato}(3-))_2\}\cdot H_2O$ in water shows a charge transfer absorption at 264 nm ($\epsilon = 4.0 \times 10^3$ M^{-1} cm^{-1}) typical of V(V) and features a broad absorption band in the visible region between 500 and 700 nm, typical of V(IV). The broad band is comprised of three absorbances at 521, 560, and 629 nm, as determined by curve fitting, with a band also appearing at 810 nm. A broad, weak band ($\epsilon < 1$ M^{-1} cm^{-1}) occurs between 900 and 1000 nm in the solution spectrum of $(NH_4)_2\{[V^V(O)_2]_2[V^{IV}(O)](\mu\text{-}(-)\text{-quinato}(3-))_2\}\cdot H_2O$, which is tentatively assigned as an intervalence transition. The diffuse reflectance spectrum of the complex dispersed in a KBr matrix shows similar features [λ_{max} (nm) = 539 sh, 646], which suggests that the integrity of the complex is maintained in solution. The electronic spectrum of $(NH_4)[V^{IV}O(HOC(Et)_2CO_2)(OC(Et)_2CO_2)]$, which contains a V(IV) center in the same coordination environment as $(NH_4)_2\{[V^V(O)_2]_2[V^{IV}(O)](\mu\text{-}(-)\text{-quinato}(3-))_2\}\cdot H_2O$, shows similar features [λ, nm (ϵ, M^{-1} cm^{-1}): 240 (1.2×10^3), 410 (30), 524 (26), 600 (24), 816 (17)],[26] except for the weak transition in the near-IR. The circular dichroism spectrum of $(NH_4)_2\{[V^V(O)_2]_2[V^{IV}(O)](\mu\text{-}(-)\text{-quinato}(3-))_2\}\cdot H_2O$ in water shows two peaks in the ultraviolet region at 284 ($\epsilon = -19.9 \times 10^{-2}$ deg M^{-1} m^{-1}) and 338 nm ($\epsilon = +7.7 \times 10^{-2}$ deg M^{-1} m^{-1}) and a broad peak between 500 and 700 nm (λ_{max}= 521 nm, $\epsilon = -1.6 \times 10^{-2}$ deg M^{-1} m^{-1}).

The single unpaired electron associated with the V(IV) center of $(NH_4)_2\{[V^V(O)_2]_2[V^{IV}(O)](\mu\text{-}(-)\text{-quinato}(3-))_2\}\cdot H_2O$ in the solid state was confirmed by magnetic susceptibility measurements; $\mu_{eff} = 1.83\ \mu_B$. This value is close to the spin only value for a d^1 system ($\mu_{so} = 1.73\ \mu_B$). The room-temperature X-band (~9.6 GHz) EPR spectrum of $(NH_4)_2\{[V^V(O)_2]_2[V^{IV}(O)](\mu\text{-}(-)\text{-quinato}(3-))_2\}\cdot H_2O$ (Figure 2) in water shows a broad eight-line signal (g_{iso} = 1.9725, $A_{iso} = 99.3 \times 10^{-4}$ cm^{-1}) as expected for a V(IV) d^1 system. The electron is largely trapped at the V(IV) center as deduced from the lack of splitting of the V(IV) EPR signal by the two terminal V(V) ions.

In the ^{13}C NMR spectra of dinuclear dioxovanadate complexes with 2-hydroxy acid ligands, **III**, significant differences between the chemical shift of the tertiary carbon of the free ligand and the respective complex (*ca.* 14 ppm) are observed due to the marked difference in the chemical environment upon bridging.[6] A smaller difference of about 5 ppm is noted for the carboxyl carbon. While the ^{13}C NMR spectrum of the quinic acid analog, **II**, also has a 5 ppm difference in chemical shift between the carboxyl carbon of the free ligand and complex (Table 5), the difference in the shift of the tertiary carbon is less marked.

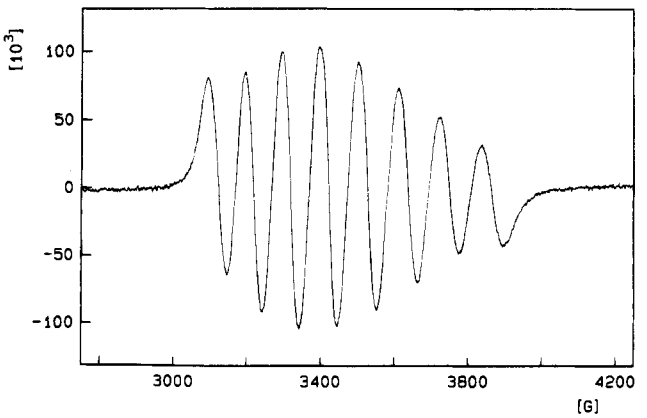

Figure 2. X-band EPR spectrum of $(NH_4)_2\{[V^V(O)_2]_2[V^{IV}(O)](\mu\text{-}(-)\text{-quinato}(3-))_2\}\cdot H_2O$ (10 mM) in water at room temperature. Conditions: sweep width 1500 G, time constant 5.12 ms, modulation amplitude 3.4 G, microwave power 0.8 mW.

Both the ^1H and ^{13}C NMR spectra of $(NH_4)_2\{[V^V(O)_2]_2[V^{IV}(O)](\mu\text{-}(-)\text{-quinato}(3-))_2\}\cdot H_2O$ are extremely broad. It is not clear whether the broadness of the signals is due to an equilibrium of species produced in solution or due to the single paramagnetic center of the complex.

Discussion

The numerous and diverse functions of vanadium in biological systems have focused research upon the coordination chemistry of vanadium to better understand its interactions with proteins. The geometries of the vanadium ions in $(NH_4)_2\{[V^V(O)_2]_2[V^{IV}(O)](\mu\text{-}(-)\text{-quinato}(3-))_2\}\cdot H_2O$ lie further toward square pyramids on the square pyramid−trigonal bipyramid continuum, with the V(IV) center having the greatest square-pyramidal character (τ = 0.17). The extra degree of trigonality of the V(V) centers approximates the coordination geometry found in the inhibitor complexes of enzymes with V(V) and uridine and is only the second structural model of the enzyme center with a coordination sphere containing a carboxylate, two oxo, and two alcoholate donors.[6a] Apart from the interest in its biomimetic structural properties, this is also the first time that a mixed-valence V(V)−V(IV)−V(V) trinuclear complex has been characterized, even though many mixed-valence dinuclear complexes and higher polynuclear complexes are known.[9] The ligand used here, quinic acid, is a useful representation of two types of biologically relevant ligands, 2-hydroxy acids and sugars. It may also be the case that sugars could form similar complexes with vanadium, in which the three donors are alcoholates, although none have been structurally characterized as yet.

It has been shown by rigorous ^1H NMR spectroscopy and energetics calculations that quinic acid (**I**) exists in the chair conformation with an equatorial carboxyl group.[7c] The crystal structure of quinic acid, recently determined, corroborates the solution conformation predictions.[25] When the carboxyl group is oriented in the equatorial plane, the hydroxyl groups on carbons 1 and 3 are in axial positions, enabling the formation of a stereochemically favored six-membered ring following deprotonation. If the carboxyl group, however, adopts an axial

(26) Barr-David, G.; Hambley, T. W.; Irwin, J. A.; Judd, R. J.; Lay, P. A.; Martin, B. D.; Bramley, R.; Dixon, N. E.; Hendry, P.; Ji, J.-Y.; Baker, R. S. U.; Bonin, A. M. *Inorg. Chem.* **1992**, *31*, 4906−4908.

position, the hydroxyl groups on carbons 1 and 3 flip into equatorial positions and are no longer potential electron donors.

The isolated dinuclear V(V) quinic acid complex, **II**, is thought to be structurally analogous to **III**. Numerous attempts to crystallize this product, however, have been unsuccessful. Where the quinic acid ligand is oriented with axial hydroxyl groups on carbons 1 and 3 as shown in **II**, it is suggested that the hydroxyl group on carbon 3 may chelate with the V(V) center, giving rise to a species with a VO^{3+} core. This formulation has quinic acid acting as a tridentate chelate as found in the trinuclear vanadium complex characterized here by crystallography. The strain in this system may also promote the oxidation of the ligand to form the mixed-valence ion. Additional resonances in the upfield region of the ^{13}C spectrum (38.9, 41.9 ppm) of **II** suggest that other species may be present in solution. The spectral pattern observed here is one that may be expected when the cyclohexane ring of the ligand flips into the alternative chair conformation, where the carboxyl group sits it an axial position. A model of such a conformation also reveals several favorable hydrogen bond interactions between the vanadium oxo groups and the hydroxyl protons. The small difference in the shift of the tertiary carbon may also be due to species where the ligand is acting as a monodentate chelate, or as a bis chelate in a nonbridging mode.

The mixed-valence V(V)−V(IV)−V(V) trinuclear complex $(NH_4)_2\{[V^V(O)_2]_2[V^{IV}(O)](\mu\text{-}(-)\text{-quinato}(3-))_2\}\cdot H_2O$ has the metal ions bridged via two tridentate quinato(3−) ligands. This trinuclear structure is able to accommodate comfortably the bulky, hydroxy-substituted cyclohexane ring. Valence-localized V(V)−V(IV) mixed-valence species are characterized by an eight-line EPR spectrum and a weak intervalence transition at approximately 1000 nm,[9] and clearly this complex fits both these criteria. The crystallographic evidence supports a valence-localized structure. If the electron were delocalized over all of the vanadium ions, a 22-line EPR spectrum would result. If it were localized on the central V(IV), an eight-line spectrum would be observed with a superimposed 15-line spectrum due to the small degree of electron density on the outer V(V) ions. The coupling to the outer V(V) centers is not observed in the EPR spectrum of the complex (Figure 2), and the signals are much broader than those observed for V(IV) monomers. This may be due to unresolved ^{51}V coupling, which will split each peak into a 15-line spectrum. If the single electron associated with the complex were delocalized over the three vanadium atoms, there would be little variation in the V−O(alcoholate) bond lengths. This, however, is not the case in the trinuclear complex under study here. The V−O (alcoholate) bonds about the V(IV) center are significantly shorter than those about the V(V) groups (V3−O3, 1.938 Å; V1−O3, 2.019 Å) which further suggests that the electron is not delocalized. The dioxo V(V) ions may require less electron density from the alcoholate donors compared to the monooxo V(IV) ion. This trend in the differing vanadium oxygen bond lengths as a function of oxidation state has been noted in a review compiling crystallographic data for a series of vanadium complexes,[24] although the phenomenon must be dependent on the electron-withdrawing/donating capacity of the ligand. A recent study of variable-valence VO^{z+} complexes with tridentate ONO and bidentate ON/NN donating ligands found that the V(IV)−O(phenolate) bond length was 0.06 Å longer than the corresponding V(V)−O(phenolate) bond.[27]

(27) Chakravarty, J.; Dutta, S.; Chandra, S. K.; Basu, P.; Chakravorty, A. *Inorg. Chem.* **1993**, *32*, 4249−4255.

Table 6. Bond Valence Sum Analysis of $(NH_4)_2\{[V^V(O_2)]_2[V^{IV}(O)](\mu\text{-}(-)\text{-quinato}(3-))_2\}\cdot H_2O$

	assumed oxidation state		
vanadium atom	V(V)[a]	V(IV)[b]	actual oxidation state
V1	5.0864	4.8318	V(V)
V3	4.4013	4.1808	V(IV)
V2	5.1006	4.8453	V(V)

[a] Presupposing the oxidation state of all vanadium ions is V(V). [b] Presupposing the oxidation state of all vanadium ions is V(IV).

The application of the bond valence sum analysis (BVSA)[28] to $(NH_4)_2\{[V^V(O)_2]_2[V^{IV}(O)](\mu\text{-}(-)\text{-quinato}(3-))_2\}\cdot H_2O$ provides additional confirmation of the mixed-valence V(V)−V(IV)−V(V) status of the complex. This analysis has been used effectively in a recent examination of the coordination environment of vanadium in bromoperoxidase.[29] Bond valences are determined according to eq 1 where B and r_0 either are

$$S = \exp[(r_0 - r)/B] \quad (1)$$

determined empirically or are determined from simple formulas and r is the experimentally determined bond length. Values of r_0 and B used in the calculations here have been obtained from Altermatt and Brown: V^{IV}−O = 1.784 Å; V^V−O = 1.803 Å; B = 0.37.[30]

The oxidation state of each vanadium as predicted by BVSA (Table 6) is in direct agreement with the actual oxidation state as determined by crystallography and from physical measurements.

Conclusion

We have isolated, characterized, and solved the crystal structure of the first mixed-valence V(V)−V(IV)−V(V) trinuclear complex, $(NH_4)_2\{[V^V(O)_2]_2[V^{IV}(O)](\mu\text{-}(-)\text{-quinato}(3-))_2\}\cdot H_2O$. The ligand utilized in the synthesis, quinic acid, is a useful model of both 2-hydroxy acids and sugars, molecules that are found in nature. The coordination geometry about each of the vanadium ions tends toward a square pyramid with the V(IV) center having the most square-pyramidal character. The diverse roles played by vanadium in the bioinorganic arena necessitates a better understanding of the coordination complexes able to be formed between vanadium and biologically-relevant ligands. The isolation of the mixed-valence V(V)−V(IV)−V(V) trinuclear complex in the current work highlights the unusual coordination possibilities for this element.

Acknowledgment. We are grateful to the Australian Research Council and the Australian Postgraduate Research Award Scheme for support and to the Australian National University Microanalytical Service for microanalysis. Assistance with the NMR experiments from Ms. Sioe-See Chew and Dr. Jacques Nemorin is also gratefully acknowledged. Access to the CD spectropolarimeter was kindly provided by Dr. R. Vagg at Macquarie University.

Supplementary Material Available: Tables S1−S6, listing H atom coordinates, expanded crystallographic details, planes, anisotropic thermal parameters, torsion angles, and close intermolecular contacts, and Figure S1, a unit cell packing diagram (18 pages). Ordering information is given on any current masthead page.

IC940981E

(28) Thorp, H. H. *Inorg. Chem.* **1992**, *31*, 1585−1588.
(29) Carrano, C. J.; Mohan, M.; Holmes, S. M.; de la Rosa, R.; Butler, A.; Charnock, J. M.; Garner, C. D. *Inorg. Chem.* **1994**, *33*, 646−655.
(30) Brown, I. D.; Altermatt, D. *Acta Crystallogr., Sect. B* **1985**, *B41*, 244−247.